Bioorganic & Medicinal Chemistry Letters 26 (2016) 1329–1332

Contents lists available at ScienceDirect

Bioorganic & Medicinal Chemistry Letters

journal homepage: www.elsevier.com/locate/bmcl

Novel morpholine scaffolds as selective dopamine (DA) D3 receptor antagonists

Fabrizio Micheli [a,*], Susanna Cremonesi [a], Teresa Semeraro [a], Luca Tarsi [a], Silvia Tomelleri [a], Paolo Cavanni [a], Beatrice Oliosi [a], Elisabetta Perdonà [a], Anna Sava [a], Laura Zonzini [a], Aldo Feriani [a], Simone Braggio [a], Christian Heidbreder [b]

[a] Aptuit s.r.l, Via Fleming 4, 37135 Verona, Italy
[b] Indivior Inc, The Fairfax Building, 10710 Midlothian Turnpike, Suite 430, Richmond, VA 23235, USA

ARTICLE INFO

Article history:
Received 23 November 2015
Revised 21 December 2015
Accepted 23 December 2015
Available online 5 January 2016

Keywords:
Dopamine
Antagonist
DA D3 receptor
7-TM
Morpholine

ABSTRACT

A new series of morpholine derivatives has been identified as selective DA D3 receptor antagonists; their in vitro profile and pharmacokinetic data are provided.

A growing number of studies have demonstrated a close association between the dopamine (DA) D3 receptor and drug addiction, which suggested that selective DA D3 receptor antagonists may be effective in reducing drug-induced incentive motivation, attenuating drug's rewarding efficacy, and reducing reinstatement of drug-seeking behavior.[1,2] Selective DA D3 receptor antagonists have been recently discovered, some with benzoazepine and [3.1.0] templates,[3,4] others with piperazine and alternative scaffolds.[5,6] The original pharmacophore model reported by Stark in 2002[7] involving the presence of a key basic moiety within the different templates used is still valid in its basic assumptions. Since then, additional evidence has been generated including X-ray structures and molecular modeling simulations.[8,9] A few examples of these templates are reported in Figure 1.

Several approaches can be used for the identification of an appropriate basic moiety that interacts with Asp$^{3.32}$ in the recently described[8] orthosteric binding site that endows the molecule with an appropriate 'anchor point' that directs the remaining part of the molecule to interact at a secondary site that is unique to D3R allowing for selectivity versus the DA D2 receptor. A combination of these approaches has been recently used[9] by exploiting the DA D3 receptor crystal structure to guide the drug design process.

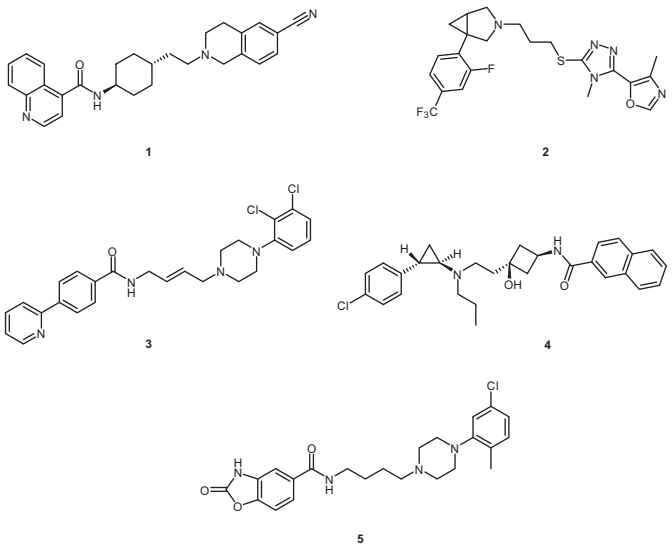

Figure 1. A few selective DA D_3 receptor antagonists. SB-277011 (**1**), GSK598809A (**2**), PG01037 (**3**), CJ-1882 (**4**), YQA14 (**5**).

* Corresponding author.

http://dx.doi.org/10.1016/j.bmcl.2015.12.081
0960-894X/

Although both affinity and selectivity are on the critical path of the drug discovery process, the overall 'developability' profile[10] of the molecule is also essential to ensure the progression of the compound toward clinical development.

This Letter describes a joint medicinal and computational chemistry 'scaffold hopping' strategy (with respect to the classical piperidines and to the azabicyclo[3.1.0]-hexanes series) that resulted in the identification of a variety of basic moieties. Specifically, a morpholine scaffold is described together with its pharmacokinetic (PK) profile.[11,12] The general structure of the newly identified DA D3 receptor antagonists is reported in Figure 2.

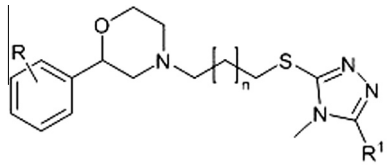

Figure 2. The general structure of the newly reported DA D3 receptor antagonist.

Biological results are reported in Tables 1–3 where **R**, **R1** and **n** refer to the general structure reported in Figure 2. Experimental details and further references for these assays can be found in Ref. 2–4.

All the compounds were prepared in agreement with Schemes 1 and 2.

All the data were compared to the affinity of SB-277011 (**1**, Fig. 1), which is one of the prototypical DA D3 receptor antagonists. The screening cascade consisted of binding affinity at the DA D3 and D2 receptors, potency of the compounds at inhibiting the human ERG potassium channel (hERG) tail current as well as

Table 1
Affinity results for the selected derivatives[a]

Entry	R	R1	n	Sterochem.	DA D3 pK_i	DA D3 GTPγS fpK_i	DA D2 pK_i	hERG fpK_i
1	N.A.	N.A.	N.A.	s.e.	8.2	8.4	6.3	6.2
6	*p*-F	4-Methyl-1,3-oxazol-5-yl	1	rac.	6.4	N.T.	<5.0	N.T.
7	*p*-F	4-Methyl-1,3-oxazol-5-yl	1	s.e.	6.6	N.T.	<5.0	5.5
8	*p*-CF_3	4-Methyl-1,3-oxazol-5-yl	1	rac.	6.9	N.T.	N.T.	N.T.
9	*p*-CF_3	4-Methyl-1,3-oxazol-5-yl	1	s.e.	7.3	7.6	4.9	5.5
10	*p*-CF_3	4-Methyl-1,3-oxazol-5-yl	2	rac.	7.1	7.6	<5.0	N.T.
11	*p*-CF_3	4-Methyl-1,3-oxazol-5-yl	2	s.e.	7.1	7.8	<5.0	5.6
12	2-F,4-CF_3	4-Methyl-1,3-oxazol-5-yl	1	rac.	6.7	N.T.	5.0	N.T.
13	*p*-CH_3	4-Methyl-1,3-oxazol-5-yl	1	rac.	6.3	N.T.	N.T.	N.T.
14	*p*-Br	4-Methyl-1,3-oxazol-5-yl	1	rac.	6.7	N.T.	4.8	N.T.
15	*p*-CF_3	Thiophen-3-yl	1	rac.	7.0	N.T.	5.1	N.T.
16	*p*-CF_3	1,3-Thiazol-2-yl	1	rac.	6.6	N.T.	5.1	N.T.
17	*p*-CF_3	1-Methyl-1*H*-pyrazol-5-yl	1	rac.	6.2	N.T.	<5.0	N.T.
18	*p*-CF_3	1-Methyl-1*H*-pyrrol-2-yl	1	rac.	6.9	N.T.	5.2	N.T.

[a] N.A. = not applicable; N.T. = not tested. Affinity results: SEM for the data sets is ±0.1. rac = racemate; s.e. = single enantiomer.

Table 2
Affinity results for the selected derivatives[a]

Entry	R	R1	n	Sterochem.	DA D3 pK_i	DA D3 GTPγS fpK_i	DA D2 pK_i	hERG fpK_i
19	*p*-CF_3	CyH	1	rac.	7.4	7.7	5.1	N.T.
20	*p*-CF_3	4-Py	1	rac.	7.0	N.T.	4.9	N.T.
21	*p*-CF_3	3-Py	1	rac.	6.6	N.T.	4.8	N.T.
22	*p*-CF_3	2-Pyrazine	1	rac.	6.8	N.T.	5.0	N.T.
23	*p*-CF_3	5-Pyridine-2-carboxamide	1	rac.	7.5	7.8	4.6	5.7
24	*p*-CF_3	5-Pyridine-3-carboxamide	1	rac.	7.0	N.T.	4.8	N.T.
25	*p*-CF_3	4-Benzeneamide	1	rac.	7.5	7.7	5.0	5.3
26	*p*-CF_3	4-Benzeneamide	1	s.e.	7.8	8.2	4.9	5.2
27	*p*-CF_3	3-Benzeneamide	1	rac.	6.5	N.T.	4.8	N.T.
28	*p*-CF_3	4-Phenylethan-1-one	1	rac.	7.2	7.7	4.7	N.T.
29	*p*-CF_3	4-Benzene-1-sulfonamide	1	rac.	6.9	N.T.	<4.5	N.T.
30	*p*-CF_3	4-Benzonitrile	1	rac.	7.0	N.T.	5.0	N.T.
31	2-F,4-CF_3	4-Benzeneamide	1	rac.	7.2	7.4	4.8	N.T.

[a] N.A. = not applicable; N.T. = not tested. Affinity results: SEM for the data sets is ±0.1. rac = racemate; s.e. = single enantiomer.

Table 3
Affinity results for the selected derivatives[a]

Entry	R	R1	n	Sterochem.	DA D3 pK_i	DA D3 GTPγS fpK_i	DA D2 pK_i	hERG fpK_i
32	*p*-CF_3	4-(1,3-Oxazol-2-yl)phenyl	1	rac.	8.3	8.0	5.8	6.0
33	*p*-CF_3	4-(1,3-Oxazol-2-yl)phenyl	1	s.e.#1	6.4	N.T.	4.8	N.T.
34	*p*-CF_3	4-(1,3-Oxazol-2-yl)phenyl	1	s.e.#2	8.2	8.5	5.3	5.9
35	*p*-CF_3	1,2,4-Triazol-4-yl)phenyl	1	rac.	6.9	N.T.	5.0	N.T.
36	*p*-CF_3	4-(1,3,4-Oxadiazol-2-yl)phenyl	1	rac.	7.8	7.9	4.9	N.T.
37	*p*-CF_3	4-(5-Methyl-1,2,4-oxadiazol-3-yl)phenyl	1	rac.	7.6	8.0	<5.0	N.T.
38	*p*-CH_3	4-(5-Methyl-1,2,4-oxadiazol-3-yl)phenyl	1	rac.	7.1	7.8	4.6	6.0

[a] N.A. = not applicable; N.T. = not tested. Affinity results: SEM for the data sets is ±0.1. rac = racemate; s.e. = single enantiomer.

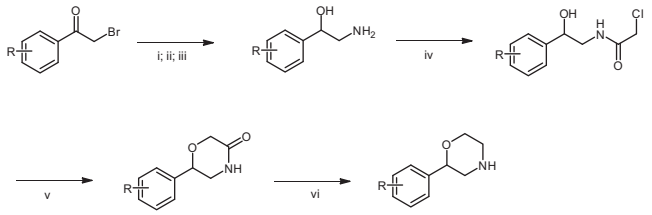

Scheme 1. Reagents and conditions: (i) HMTA, $CHCl_3$, 16 h, rt; (ii) 37% HCl, EtOH, 12 h, rt; (iii) $NaBH_4$, MeOH, 30 min, 0 °C; (iv) chloroacetylchloride, TEA, DCM, 1 h, 0 °C; (v) *t*-BuOK, THF, 1 h, 0 °C—rt; (vi) $LiAlH_4$, THF, 1 h, reflux.

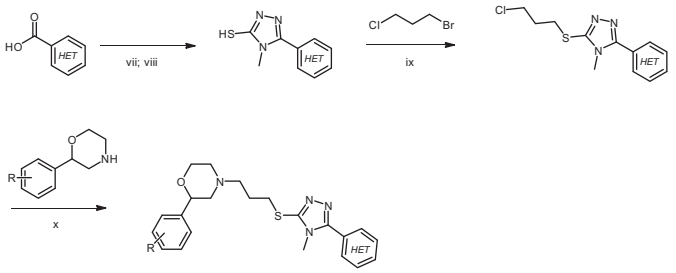

Scheme 2. Reagents and conditions: (vii) T3P in AcOEt, 4-methyl-3-thiosemicarbazide, DIPEA, DMF, 12 h, rt; (viii) 4 M NaOH, 40 min, reflux; (ix) K_2CO_3, methanol/acetone, 12 h, rt; (x) Na_2CO_3, NaI, DMF, 12 h, 60 °C.

selectivity of this new class versus the DA D1 and D4 receptors, and Muscarinic M1 and M3 receptors.

All the compounds with $pK_i > 7.0$ were tested to evaluate their functional activity. No sign of agonism at the DA D3 receptor was observed ($fpK_i < 5$ for all the compounds tested) while the antagonistic fpK_i values are reported in Tables 1–3.

Selected compounds went through generic developability screens such as CYPEX bactosome P450 inhibition and rat and human in vitro clearance in liver microsomes early in the screening cascade to predict their PK and developability profiles.

The first compound identified during this 'scaffold hopping' exercise was the racemic derivative **6**, which showed micromolar affinity at the DA D3 receptor. The mixture was therefore separated by chiral HPLC and the most potent enantiomer (**7**) was evaluated. In terms of selectivity, this compound was completely inactive at the DA D1, DA D4 and at the M3 receptors, showing functional pK_i (fpK_i) = 5.5 at the M1 receptor. A 10-fold difference with hERG electrophysiological measure was also observed.

From a developability point of view, compound **7** showed IC_{50} values greater than 30 μM on all CYP P450 isoforms tested (namely CYP1A2, CYP2C9, CYP2C19, CYP2D6, CYP3A4 DBOMF and CYP3A4 7BQ), low-moderate clearance in human (hCli = 21.7 μL/min/mg protein), and low clearance in rat (rCli) (<9 μL/min/mg protein) microsomes.

In order to fully assess the potential of the scaffold, its properties were further explored in vivo[11] in a portal vein-cannulated rat model.[12] Compound **7** had 100% fraction absorbed (Fa%), low distribution volume (V_{ss} = 2.6 l/kg), and moderate clearance as expected from the in vitro parameters (Clb = 40.0 mL/min/kg) leading to a relatively short half-life ($T_{1/2}$ = 0.8 h). Nonetheless, hepatic extraction (Eh) was low (Eh = 0.1) resulting in almost full 100% bioavailability. The percentage of fraction unbound (Fu%) in blood and plasma was also measured with 17% of the compound in free form in blood; in the brain this compound was present as 'free' for more than 50%.

The importance of 'developability' and 'drug efficiency',[13] led quite naturally to the next exploration step that focused on replacing the fluorine atom present on the aromatic ring of compound **6** with a trifluoromethyl group, resulting in the racemate **8** and in the

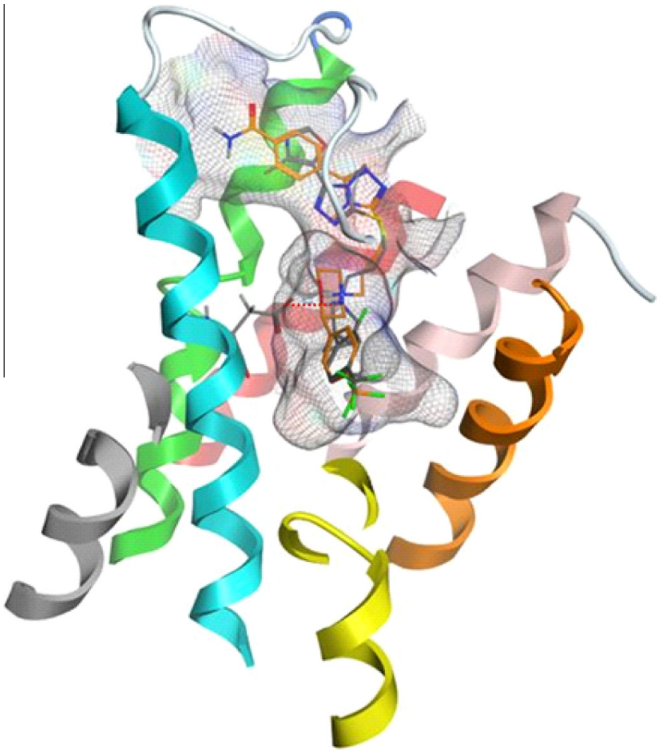

Figure 3. Derivative **26** (orange) fitted in the DA D3 receptor model together with **2** (atom type). The interaction between the basic nitrogen of the morpholine or [3.1.0] hexane moieties and $Asp^{3.32}$ is clearly visible (red dotted line).

active enantiomer **9**. This substitution led to approximately 10-fold increased affinity at the DA D3 receptor, 100-fold selectivity over the DA D2 receptor, and more than 50-fold selectivity over the hERG channel. This substitution had no effect on the affinity at DA D1 and D4 receptors ($pK_i < 4.0$), but resulted in a slight increase in affinity at the M1 and M3 receptors ($fpK_i = 6$). Increased inhibition of CYP P450 was observed with this compound, which showed IC_{50} values greater than 6 μM on all isoforms tested. A slight increase in the in vitro clearance in human (hCli = 40.0 μL/min/mg protein) with no observed changes in rat microsomes. This compound also showed Fa% = 63%, V_{ss} = 2.5 (l/kg), and Clb = 13.5 (mL/min/kg) leading to $T_{1/2}$ = 3.5 (h); Eh was low (0.1) leading to 58% bioavailability. The percentage of fraction unbound in blood and plasma was definitely lower with blood Fu% equal to 6.2% and brain Fu% equal to 7.1%. This decrease might be linked to the increased overall lipophilicity (*c*Log*P* from 2.13 to 2.87)[14] due to the introduction of the $-CF_3$ moiety.

Increasing the length of the linker portion from 3 to 4 carbon atoms (racemic derivative **10** and its enantiomer **11**) had no major impact on the primary pharmacological profile.

The introduction of an additional fluorine atom on the aromatic ring linked to the morpholine moiety (**12**) led to slightly reduced affinity at the DA D3 receptor. Replacement of the $-CF_3$ with a methyl group (**13**) resulted in decreased affinity at the DA D3 receptor, while a 4-bromine alone (**14**) was almost identical to the 2-F, 4-CF_3 substitution.

The next steps of the exploration focused on the heteroaromatic portion of the scaffold, where the methyl oxazole was initially replaced by a thiophene moiety (**15**) with similar affinity to **8**. The introduction of a nitrogen atom (thiazole-2-yl, **16**) resulted in decreased affinity at the DA D3 receptor, which was even worse with the methyl-pyrazol-5-yl derivative **17**. In contrast, a single nitrogen atom (methyl-pyrrol-2-yl) **18** was very similar to the original derivative **8**.

The results of the next exploration are reported in Table 2.

Additional exploration sought to further improve the SAR and consolidate our knowledge of the DA D3 receptor. The complete removal of the R1 aromatic ring and its replacement with a lipophilic cyclohexane (**19**, Table 2) resulted in a 200-fold selective compound versus DA D2 receptor, but with very high lipophilicity (*c*Log*P* = 5.1).[14] The introduction of a 4-pyridyl ring (**20**) achieved the desired 100-fold selectivity versus DA D2 receptor, but with lower *c*Log*P* (3.7). In contrast, moving the pyridine nitrogen in position 3 (**21**) had a detrimental effect on the primary affinity at the DA D3 receptor, leading to half-log unit loss; the same held true with the introduction of a 2-pyrazine moiety (**22**). A carboxamide moiety was then introduced to further reduce *c*Log*P*. Derivative **23** (*c*Log*P* = 2.9) not only achieved a very high selectivity versus DA D2 receptor (800-fold), but was also assayed versus hERG channel with about 60-fold selectivity. Modification of the nitrogen position of the pyridine scaffold (**24**) reduced the affinity at the DA D3 receptor, while its complete removal and the transformation into a benzamide moiety (**25**) maintained the affinity at the DA D3 receptor and resulted in 150-fold selectivity versus hERG channel. This compound was completely inactive at the DA D1, DA D4 and M3 receptors, and had 30-fold selectivity over the M1 receptor (fpK_i = 6.0). The single enantiomer (**26**) was even better with 400-fold selectivity over the hERG channel; its Cli in rat was 16.3 while Cli in human was 63.2 (μL/min/mg protein). This compound had IC_{50} values greater than 30 μM on all CYP P450 isoforms tested, while its brain Fub% was 3.0% and blood Fub% 4.5%.

A change in the position of the amide (**27**) was detrimental to the affinity at the DA D3 receptor, while the transformation in an acetyl group (**28**) seemed well tolerated. The primary sulfonamide (**29**) was slightly less active and comparable to the benzonitrile (**30**). The introduction of a fluorine atom in position 2 on the aromatic ring holding the $-CF_3$ portion (**31**) produced a compound that was slightly less active than derivative **25**, but with increased lipophilicity (*c*Log*P* = 3.9).

The synthesis of bi-aryl derivatives was initiated to complete the initial exploration of this new class and to understand how much space was really available in the receptor around the morpholine moiety (Fig. 3).[15] Results are reported in Table 3.

The first attempt introduced a phenyl as a spacer before a known and tolerated oxazole moiety (**32**). Despite the obvious increase in *c*Log*P* (4.8), the compound showed unexpected increased affinity at the DA D3 receptor resulting in 300-fold selectivity versus DA D2 receptor and 200-fold selectivity versus hERG channel. This profile was also characterized by a clear stereo-differentiation of potency between the two enantiomers as clearly illustrated by derivatives **33** (enant. #1) and **34** (enant. #2). The increase in lipophilicity, however, decreased the developability potential of derivative **34**, which showed rat and human Cli of 113.7 and 668.0 (μL/min/mg protein), respectively. This compound had IC_{50} values greater than 3 μM on all CYP P450 isoforms tested, while its Fub% in brain and blood was 0.5% and 0.8%, respectively.

The introduction of a triazolyl moiety (**35**) clearly demonstrated that lipophilicity (*c*Log*P* = 2.7) is manageable in this series even if the affinity at the DA D3 receptor dropped more than 10-fold with respect to derivative **32**.

The oxadiazole **36** was somehow intermediate both in terms of affinity (pK_i = 7.8) and lipophilicity (*c*Log*P* = 3.9), while **37** resulted in improved DA D2 selectivity with a slightly reduced affinity at the DA D3 receptor despite higher *c*Log*P* (5.1). Another important factor to be considered is the role played by the position of the substituents in such a crowded space as demonstrated by compound **38** (pK_i = 7.1; cLogP = 4.7) where a substitution ($-CH_3$ vs $-CF_3$) on the other side of the molecule exemplified the difference with derivative **37**.

In conclusion, a joint computational-medicinal chemistry 'scaffold hopping' strategy resulted in the discovery of novel, selective and developable DA D3 receptor antagonists. The lead optimization of this new class is currently ongoing, while other scaffolds derived from the same exercise will be presented in the near future.

Acknowledgments

We would like to acknowledge Indivior for supporting this project as well as all relevant Aptuit departments involved in the data generation process.

References and notes

1. (a) Heidbreder, C. A.; Newman, A. H. *Ann. N.Y. Acad. Sci.* **2010**, *1187*, 4; (b) Heidbreder, C. *CNS Neurol. Disord.: Drug Targets* **2008**, *7*, 410; (c) Newman, A. H.; Blaylock, B. L.; Nader, M. A.; Bergman, J.; Sibley, D. R.; Skolnick, P. *Biochem. Pharmacol.* **2012**, *84*, 882; (d) Heidbreder, C. *Naunyn-Schmiedeberg's Arch. Pharmacol.* **2013**, *386*, 167.
2. (a) Micheli, F. *ChemMedChem* **2011**, *6*, 1152; (b) Micheli, F.; Heidbreder, C. *Expert Opin. Ther. Pat.* **2013**, *23*, 363; (c) Micheli, F.; Heidbreder, C. A. *Expert Opin. Ther. Pat.* **2008**, *18*, 821.
3. Micheli, F.; Bonanomi, G.; Blaney, F. E.; Braggio, S.; Capelli, A. M.; Checchia, A.; Curcuruto, O.; Damiani, F.; Di-Fabio, R.; Donati, D.; Gentile, G.; Gribble, A.; Hamprecht, D.; Tedesco, G.; Terreni, S.; Tarsi, L.; Lightfoot, A.; Pecoraro, M.; Petrone, M.; Perini, O.; Piner, J.; Rossi, T.; Worby, A.; Pilla, M.; Valerio, E.; Griffante, C.; Mugnaini, M.; Wood, M.; Scott, C.; Andreoli, M.; Lacroix, L.; Schwarz, A.; Gozzi, A.; Bifone, A.; Ashby, C. R., Jr.; Hagan, J. J.; Heidbreder, C. *J. Med. Chem.* **2007**, *50*, 5076.
4. Micheli, F.; Arista, L.; Bonanomi, G.; Blaney, F. E.; Braggio, S.; Capelli, A. M.; Checchia, A.; Damiani, F.; Di Fabio, R.; Fontana, G.; Gentile, G.; Griffante, C.; Hamprecht, D.; Marchioro, C.; Mugnaini, M.; Piner, J.; Ratti, E.; Tedesco, G.; Tarsi, L.; Terreni, S.; Worby, A.; Ashby, C. R., Jr.; Heidbreder, C. *J. Med. Chem.* **2010**, *53*, 374.
5. Chen, J.; Levant, B.; Jiang, C.; Keck, T. M.; Newman, A. H.; Wang, S. *J. Med. Chem.* **2014**, *57*, 4962.
6. Hua, R.; Song, R.; Yang, R.; Su, R.; Li, J. *Eur. J. Pharm.* **2013**, *720*, 212.
7. Hackling, A. E.; Stark, H. *ChemBioChem* **2002**, *3*, 946.
8. Newman, A. H.; Beuming, T.; Banala, A. K.; Donthamsetti, P.; Pongetti, K.; LaBounty, A.; Levy, B.; Cao, J.; Michino, M.; Luedtke, R. R.; Javitch, A.; Shi, L. *J. Med. Chem.* **2012**, *55*, 6689.
9. Keck, T. M.; Burzynski, C.; Shi, L.; Newman, A. H. *Adv. Pharmacol. (San Diego, CA, United States)* **2014**, *69*, 267. Emerging Targets & Therapeutics in the Treatment of Psychostimulant Abuse.
10. (a) Hughes, J. P.; Rees, S.; Kalindjian, S. B.; Philpott, K. L. *Br. J. Pharmacol.* **2011**, *162*, 1239; (b) Saxena, V.; Panicucci, R.; Joshi, Y.; Garad, S. *J. Pharm. Sci.* **2009**, *98*, 1962; (c) Han, C.; Wang, B. In *Drug Delivery Principles and Applications*; Wang, B., Siahaan, T., Soltero, R., Eds.; John Wiley & Sons, 2005. ISBN: 0-471-47489-4, Chapter 1.
11. The research complied with national legislation and with company policy on the Care and Use of Animals and with related codes of practice.
12. Matsuda, Y.; Konno, Y.; Satsukawa, M.; Kobayashi, T.; Takimoto, Y.; Morisaki, K.; Yamashita, S. *Drug Metab. Dispos.* **2012**, *40*, 2231.
13. Braggio, S.; Montanari, D.; Rossi, T. *Expert Opin. Drug Discov.* **2010**, *5*, 609.
14. Marvin Sketch Version: 6.1.7 (Chemaxon).
15. A model of the DA D3 receptor (D3R) X-ray crystal structure (PDB ID 3PBL), pre-treated using 'Structure Preparation application' within MOE,[16] was built in agreement with the simulation results, supported by experimental data, reported in Ref. 8. The secondary binding pocket (SBP) of the D3R Ptm23 (subpocket of SBP at the interface of TM2, TM3, EL1 and EL2) was created modifying the Prokink wobble angle of the TM2 Pro84 using the capabilities included in the 'protein modeling' module within MOE. Standards compounds (**1**–**5**) were docked in the minimized model, by a pharmacophore guided induced fit docking protocol, consisting in an H bond donor (to Asp110) and an aromatic center (located into the Ptm23 pocket) features as placement constraints. Ambe12: EHT and 'Reaction field' were used, respectively, as force field and implicit solvent model. Best poses were further submitted to conformational search using LowModeMD simulation (MOE) in order to optimize extracellular loops interaction (in particular EL1).
16. Molecular Operating Environment (MOE), 2013.08; Chemical Computing Group Inc., 1010 Sherbooke St. West, Suite #910, Montreal, QC, Canada, H3A 2R7; 2015.